

# Characterization of Hygroscopic Swelling Behavior of Mold Compounds and Plastic Packages

Eric Stellrecht, Bongtae Han, *Member, IEEE*, Michael Pecht, *Fellow, IEEE*

**Abstract**— **Hygroscopic swelling behavior of mold compounds is analyzed by a novel experimental procedure using a whole-field displacement technique. Large variation in moisture content at the virtual equilibrium state is observed, while the coefficient of hygroscopic swelling is shown to not vary significantly. An investigation on an actual package is also performed to determine the hygroscopic swelling mismatch strains at the chip/mold compound interface. The results are compared with the thermal expansion mismatch strains at the same interface and reveal much higher hygroscopic swelling mismatch strains. The hygroscopic strains must be considered for reliability assessment when a package is subjected to environments where the relative humidity fluctuates.**

**Index Terms** – **Chip/mold compound interface, humidity, hygroscopic swelling behavior, mold compounds, plastic encapsulated microcircuit (PEM).**

## I. INTRODUCTION

A plastic encapsulated microcircuit (PEM) consists of a silicon chip, a metal support or leadframe, wires that electrically attach the chip's circuits to the leadframe, and a plastic epoxy encapsulating material, or mold compound, to protect the chip and the wire interconnects [1]. The mold compound is a composite material made up of an epoxy matrix that encompasses silica fillers, stress relief agents, flame-retardants, and many other additives.

In spite of many advantages over hermetic packages in terms of size, weight, performance, and cost, one important disadvantage of PEMs is that the polymeric mold compound absorbs moisture when exposed to a humid environment. Moisture absorption is caused by the polymer-water affinity action. The action occurs due to the availability of hydrogen

bonding sites along the polymer chains that constitute the molding compound [2],[3]. Two distinct states of water have been identified to exist within a polymeric material. The first, called "free" or "unbound" volume, is attributed to water molecules that group in voids in the material. The second, called "bound" volume, describes water molecules that form hydrogen bonds with the polymer chains [2]-[6].

It has been shown that the swelling efficiency [2], defined as the ratio of hygroscopic volume of expansion to the volume of absorbed liquid water, is less than one. This implies that not all of the absorbed moisture contributes to the swelling of the mold compound, and it has been speculated that only the bound volume contributes to hygroscopic swelling. More specifically, the polar water molecules form hydrogen bonds with the hydroxyl groups in the mold compound and disrupt inter-chain hydrogen bonding. These water molecules effectively increase the inter-segmental hydrogen bond length and collectively cause the polymeric material to swell [2],[6],[7].

Hygroscopic stresses arise in an electronic package when the mold compound and other polymeric materials swell upon absorbing moisture while the adjacent non-polymeric materials, such as the lead frame, die paddle, and silicon chip, do not experience swelling. The differential swelling that occurs between the mold compound and non-polymeric materials leads to hygroscopic mismatch stresses in the package [2],[8],[9].

This study characterizes the hygroscopic swelling properties of five different types of mold compounds by a novel experimental procedure. The procedure utilizes a real-time whole-field displacement measurement technique called *moiré interferometry*, to conduct extremely accurate measurements. The technique is used subsequently to investigate the deformations of an actual package, caused by the mismatch in hygroscopic swelling. The hygroscopic deformation is compared with the thermal deformation and its implications are discussed.

## II. HYGROSCOPIC SWELLING

### A. Experimental Method

An experimental procedure to document hygroscopic swelling in mold compounds using *moiré interferometry* is described here. Additional details concerning the experimental procedure can be found in [9].

Manuscript received December 1, 2003; revised February 17, 2004. This work was supported by the CALCE Electronic Product and Systems Center, University of Maryland. This work was recommended for publication by Associate Editor L.T. Nguyen upon the evaluation of the reviewers' comments.

Eric Stellrecht is with the Mechanical Engineering Department, DRS Electronic Warfare and Network Systems, Inc., Buffalo, NY 14225 USA (e-mail: estellrecht@drs-ewns.com).

Bongtae Han and M.G. Pecht are with the CALCE Electronic Products and Systems Center, Department of Mechanical Engineering, University of Maryland, College Park, MD 20742 USA.

Digital Object Identifier 10.1109/TCAPT.2004.831777

1) Real-Time Moiré Interferometry

Moiré interferometry measures in-plane displacements with very high sensitivity. It has been practiced extensively in the microelectronics industry to measure the thermally induced deformation of electronic packages [10]-[13],[17].

In this method, a high-frequency cross-line grating is replicated on the specimen, initially of frequency  $f_s$ , and deforms together with the specimen. Two mutually coherent beams of laser light form a virtual reference grating, which interacts with the deformed specimen grating to produce moiré fringe patterns. These moiré patterns are contour maps of the  $U$  and  $V$  displacement fields, i.e., the displacements in the  $x$  and  $y$  directions, respectively, of each point in the specimen grating. The relationships, for every  $x,y$  point in the field of view, are

$$U(x,y) = \frac{1}{2f_s} N_x(x,y) \tag{1}$$

$$V(x,y) = \frac{1}{2f_s} N_y(x,y)$$

In routine practice of moiré interferometry,  $f_s = 1200$  lines/mm. In the fringe patterns, the contour interval is  $1/2f_s$ , which is  $0.417 \mu\text{m}$  displacement per fringe order.

For hygroscopic swelling measurements, deformations are documented at an elevated temperature. Therefore, it is necessary to implement moiré interferometry with an environmental chamber that provides convection heating and cooling. The air inside the chamber must be circulated vigorously to maintain the constant temperature. Consequently, the environmental chamber experiences vibrations that are normally transmitted to the specimen. Moiré interferometry measures tiny displacements and those inadvertent vibrations cause the moiré fringes to dance at the vibration frequency.

A compact real-time moiré setup that circumvents the vibration problem is employed in the experiment [14]. Two major components in this setup are a portable moiré interferometer (PEMI II, Photomechanics Inc.) and a computer controlled environmental chamber (EC1A, Sun Systems). As illustrated in Fig. 1, the specimen holder is not attached to the chamber. Instead, it is connected directly to the interferometer and it becomes essentially free from the environmental chamber. Furthermore, the interferometer and the chamber are mounted on separate tables and thus the interferometer is mechanically isolated from the chamber. With this arrangement, moiré fringes can be recorded while the chamber is being operated. Further details of the rod assembly and the temperature control can be found in Ref. [14].

2) Measurement Procedure

The overview of the experimental procedure is illustrated in Fig. 2. Two samples of a particular mold compound (~2mm thick) were first subjected to a 125°C bake for a minimum of 100 hours to remove any initial moisture that may have existed in the samples; (a). The bake time was determined by periodically monitoring the weights of the samples (using a Mettler AE100 analytical balance with a resolution of 0.1 mg)

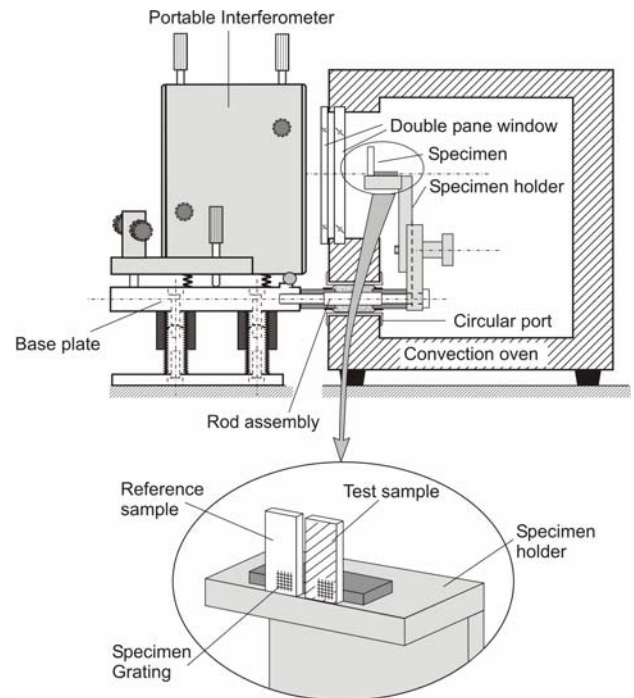


Fig. 1 Experimental apparatus for real time observation of moiré fringes [9].

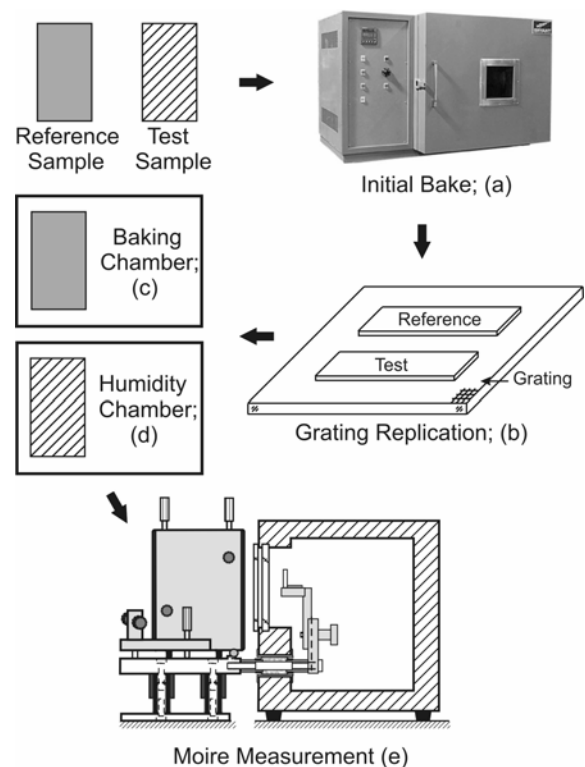


Fig. 2. Overview of experimental procedure.

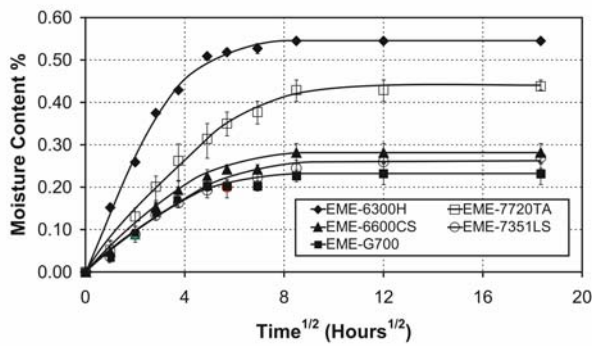


Fig. 3. Sorption curves of mold compounds.

until the measured weight of each sample remained unchanged for an extended period of time.

When the bake was completed, the samples were temporarily removed from the baking oven and a cross-line diffraction grating was replicated onto the samples at an elevated temperature of 85°C using a high temperature curing epoxy (Tra-Con Tra-Bond F230); (b). The detailed procedure of grating replication can be found in detail in [10][11][12].

One of the two samples was selected and left in the baking oven to ensure no extra moisture gain; (c). This sample was referred to as the *reference sample*. The second sample, referred to as the *test sample*, was subjected to an 85°C/85%RH environment and its weight is periodically monitored until a virtual saturation state was reached; (d). The virtual saturation state is defined as the occurrence of no additional weight gain within the resolution of the balance for two to three days.

The sorption curves of the five mold compounds are shown in Fig. 3. Once the virtual saturation state was achieved, the hygroscopic swelling measurement was performed by moiré interferometry during desorption process; (e).

It is vital to eliminate thermal expansion during moiré measurements so that only hygroscopic swelling is documented. This was accomplished by using the reference sample. As illustrated in the insert of Fig. 1, the reference and test samples were positioned side by side within the viewing area of the moiré setup. The interferometer was first tuned to produce a null field (devoid of fringes) on the reference sample and the test sample was viewed subsequently. This procedure canceled any thermally induced deformations in the test sample since the deformed state of the reference sample was used as a reference datum for zero hygroscopic deformation of the test sample. It is important to note that the specimen grating, which consisted of thin layers of gold and epoxy, had virtually no influence on the absorption and desorption characteristics of the samples [9].

*B. Hygroscopic Swelling Coefficient*

The above procedure was used to analyze five mold compounds, manufactured by Sumitomo Bakelite Co., Ltd. The material properties are shown in Table 1. The measurement was repeated on three different samples of each mold compound to ensure repeatability.

Properties	EME-6300H	EME-7720TA	EME-6600CS	EME-7351LS	EME-G700
Ash Content (wt. %)	70-73	84-88	80-83	85-89	85-89
Filler Ratio (spherical/flake)	50/50	100/0	70/30	100/0	100/0
Filler Particle Size (microns)	25-31	15-21	13-18	10-16	10-20
Epoxy Type	O-Cresol Novolac (OCN)	Multi-Func.	Di Cyclo Penta Diene (DCPD)	Biphenyl	Multi Aromat.
Hardener	Phenol Novolac (PN)	Multi-Func.	Phenol Novolac (PN)	Elastic	Multi Aromat.
Thermal Expansion, $\alpha_1$ (ppm/°C)	17	13	11	10	12
Thermal Expansion, $\alpha_2$ (ppm/°C)	68	40	50	42	49
$T_g$ (°C)	165	195	165	135	130

Table 1. Properties of the 5 mold compounds

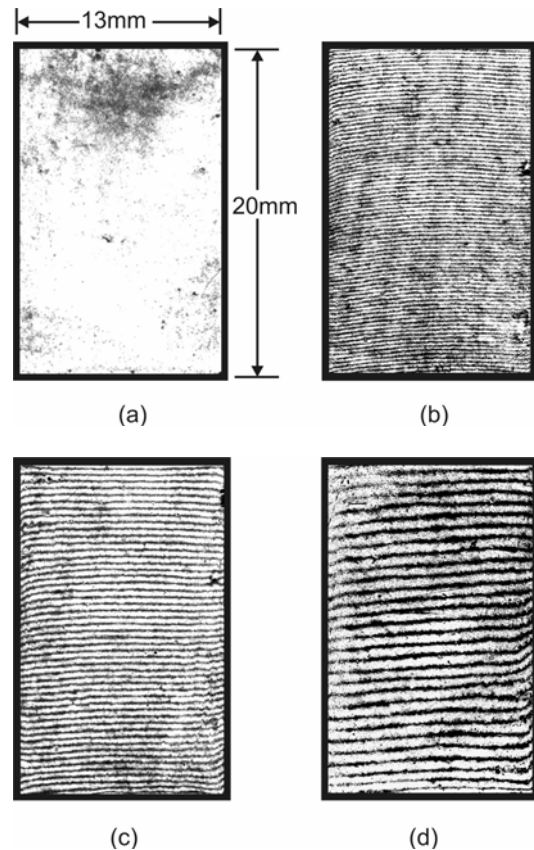


Fig. 4. V field moiré patterns obtained from mold compound EME-7720TA. (a) Null field obtained from the reference sample; fringe patterns of the test sample at time intervals of (b) zero, (c) sixteen, and (d) four-hundred hours.

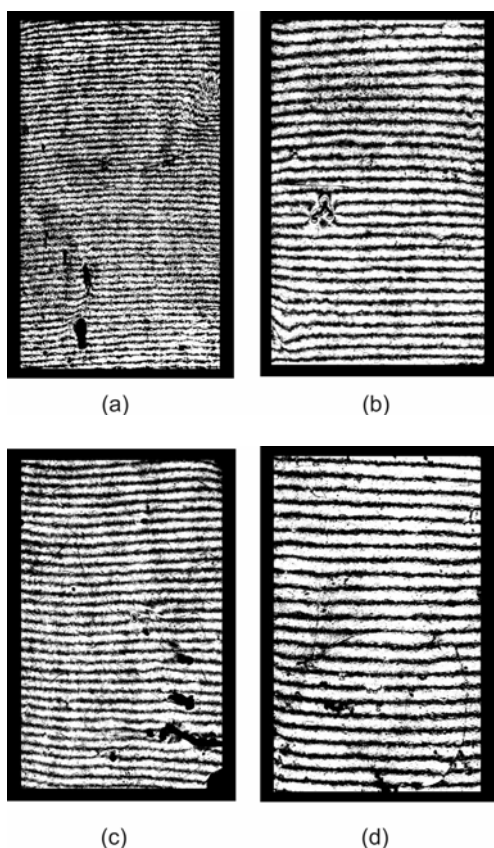


Fig. 5 V field moiré patterns obtained from other mold compounds at the virtual saturation state (time zero); (a) EME-6300H (b) EME-6600CS (c) EME7351LS and (d) EME-G700.

The V field fringe patterns of EME-7720TA obtained during the desorption process are shown in Fig. 4. The null field pattern of the reference sample is shown in (a), and the fringe patterns of the test sample at time intervals of zero, sixteen, and four hundred hours are shown in (b), (c) and (d), respectively. The test specimen contracted as desorption progressed, as evidenced by a decrease in the number of fringes in the patterns. The fringe patterns at the zero hour (Fig. 4b) represent the hygroscopic swelling at the virtual saturation point. The V field fringe patterns of the other mold compounds obtained at the virtual saturation point (at the zero hour) are shown in Fig. 5.

It is worth noting that the pattern at four hundred hours (Fig. 4d) has a few residual fringes. These residual fringes were produced by a small amount of moisture (0.04 to 0.08%) that remained in the mold compounds after the desorption process [9,15]. If the specimen had returned to its original "dry" condition, the pattern would have been devoid of fringes. This condition was observed for all five mold compounds. It was speculated that the small amount of residual moisture might be attributed to the lower desorption temperature (85°C) compared with the bake temperature (125°C).

The hygroscopic strain,  $\epsilon_h$ , can be determined directly from moiré fringe patterns by

$$\epsilon_h = \frac{1}{2f_s} \frac{\Delta N}{\Delta L} \quad (2)$$

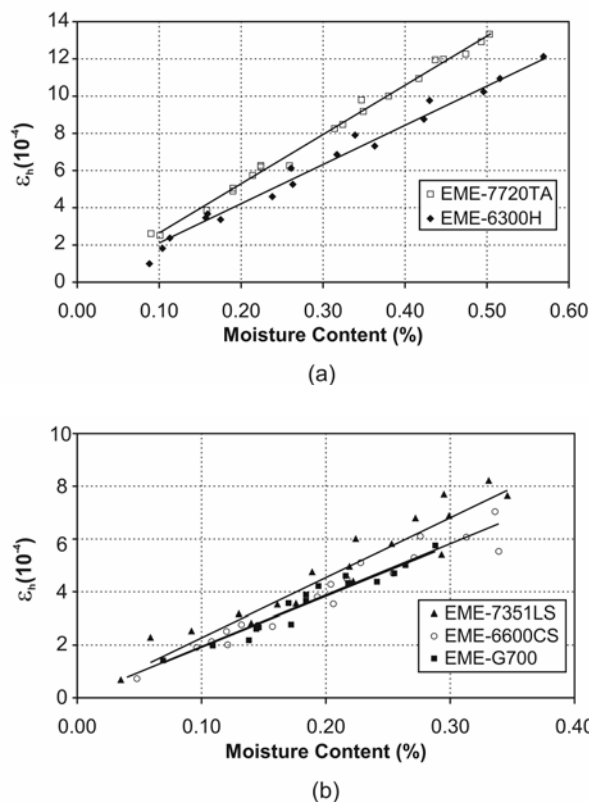


Fig. 6 Hygroscopic strain vs. moisture content (%) obtained from the moiré fringes.

where  $f_s$  is the frequency of the specimen grating (1200 lines/mm),  $\Delta N$  is the change of fringe orders in the moiré pattern and  $\Delta L$  is any gage length across which  $\Delta N$  is determined.

The V field hygroscopic strains are plotted against moisture content (%) in Fig. 6. It is evident that a linear relationship exists between hygroscopic swelling and moisture content. The constant of linearity, called the *coefficient of hygroscopic swelling (CHS)* [9], is defined as

$$\beta = \frac{\epsilon_h}{\%C} \quad (3)$$

where  $\beta$  is the CHS and %C is the moisture content percentage calculated by  $\%C = \frac{Wet\ weight - Dry\ weight}{Dry\ weight} \times 100$ . "Wet

weight" is defined as the weight of the sample including the weight of the absorbed moisture. The CHS is a material property of the mold compound and, if known, the hygroscopic swelling can be determined by measuring the moisture content in the mold compound.

The test results are summarized in Table 2, which includes CHS values, virtual equilibrium moisture content and the corresponding hygroscopic swelling obtained from Eq. 3. Although only V field fringes were shown in Figs. 4, and 5, the corresponding U field patterns were documented and both fields were used to determine the CHS values. The average CHS value of the five mold compounds is 0.22. The variation of the CHS value is less than 20%. However, the maximum moisture content shows significant variation, which is

Properties	EME-6300H	EME-7720TA	EME-6600CS	EME-7351LS	EME-G700
Average CHS (% $\epsilon_h$ /%C)	0.21	0.26	0.21	0.24	0.19
Virtual Equilibrium Moisture Content (%C)	0.54	0.45	0.29	0.26	0.24
Hygroscopic Swelling (% $\epsilon_h$ )*	0.11	0.12	0.06	0.06	0.05
CTE (ppm/°C)	17	13	11	10	12
Temperature Excursion (°C)	65	92	55	60	42
Thermal Mismatch Strain (%)**	0.14	0.10	0.08	0.07	0.09

\* for 85°C/85%RH

\*\* for  $\Delta T=100^\circ\text{C}$

Table 2. Experimental results.

attributed to the combined effect of the amount of ash content and the resin/hardener system. The moisture content of the first two mold compounds (EME-6300H and EME-7720TA) is nearly twice as large as that of the other three mold compounds (EME-6600CS, EME-7351LS and EME-G700). Consequently, the first two mold compounds exhibit almost twice the hygroscopic swelling compared to that of the other three compounds.

### III. COMPARISON BETWEEN HYGROSCOPIC AND THERMAL DEFORMATIONS

The temperature excursion required to produce a thermal expansion equal to the hygroscopic swelling in the mold compound specimen can be calculated by:

$$\Delta T = \frac{\epsilon_h}{\alpha} = \frac{\beta \cdot C}{\alpha} \quad (4)$$

where  $\alpha$  is the coefficient of thermal expansion (CTE) in ppm/°C. This comparison is shown in the lower half of Table 2. The deformation caused by hygroscopic swelling can be as significant as the thermal deformation caused by  $\Delta T$  of 92°C.

If a mold compound/silicon chip assembly is considered, the hygroscopic mismatch strain component in the direction of the mold compound/chip interface would be identical to hygroscopic swelling in the mold compound at the interface, because the chip does not absorb moisture and does not swell. Assuming that the chip does not deform the thermal mismatch strains,  $\epsilon^\sigma$ , can be approximated as:

$$\epsilon^\sigma = (\alpha_{\text{mold compound}} - \alpha_{\text{chip}}) \Delta T. \quad (5)$$

The results are shown in the last row of Table 2, where the chip CTE of 3 ppm/°C and a temperature excursion of 100°C were used. The hygroscopic mismatch strains are compatible with the thermal strains induced by the considerable thermal excursion.

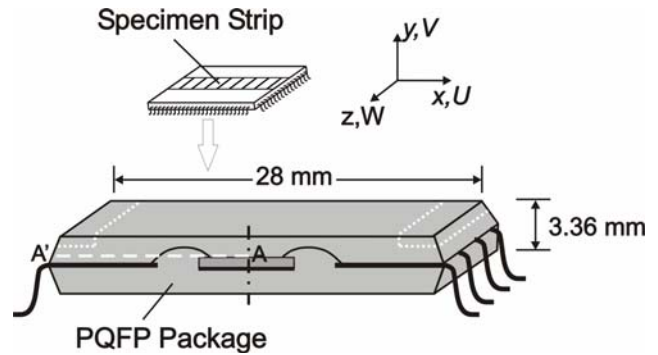


Fig. 7. PQFP package for moiré experiments. The CTE and CHS of the mold compound of the package were determined from the regions marked by dashed boxes.

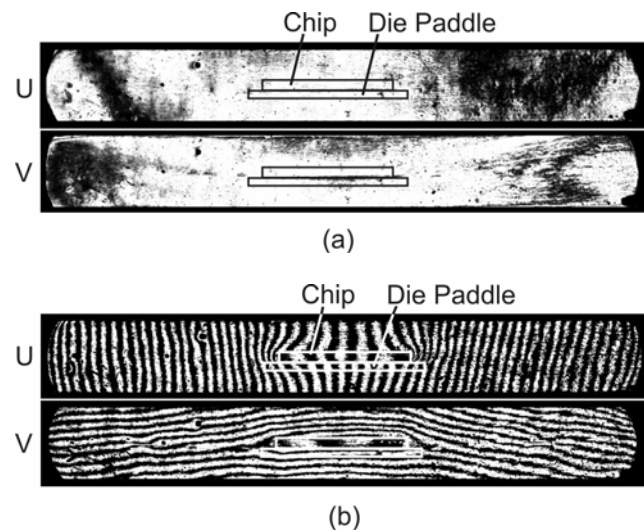


Fig. 8. (a) Null field patterns documented at 85°C before moisture absorption, and (b) fringe patterns induced by cooling the package to 25°C ( $\Delta T=-60^\circ\text{C}$ ).

The experimental results presented here imply that the hygroscopic swelling would play an important role in the cycles-to-failure of the package when the package is subjected to environments where the relative humidity fluctuates. The experimental technique was used to investigate the stress induced deformation of an actual package. This has not been possible with the measurement techniques employed in the previous studies of hygroscopic swelling, which were virtually point-measurement techniques. The results are reported in the following section.

### IV. ANALYSIS OF PLASTIC QUAD FLAT PACKAGE

The package selected for the test was a square quad flat plastic package with 100 I/O's. The package contained a copper lead-frame and a chip with dimensions of 6.36 x 6.36 x 0.5 mm. The package was prepared as shown in Fig. 7 to investigate the interaction between the mold compound and the chip. The opposing sides of the package were trimmed and ground using a precision grinding machine until the

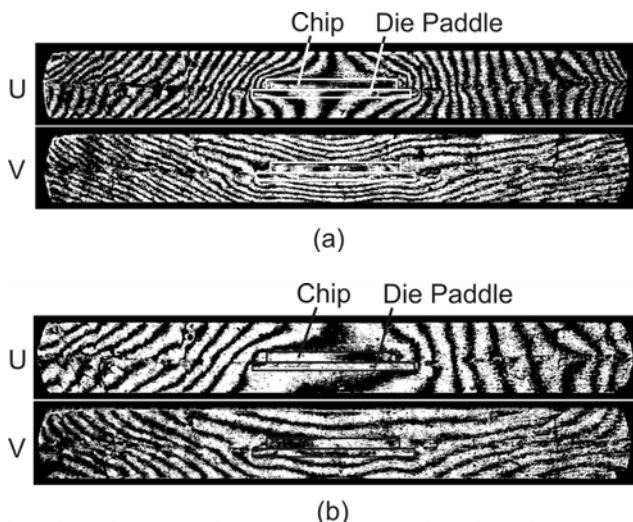


Fig. 9. Fringe patterns obtained at 85°C during desorption process; (a) at its virtual equilibrium state and (b) after 8 hours.

silicon chip was exposed on both sides. This specimen configuration preserved the symmetric boundary conditions. After the existing moisture was removed by baking at 125°C, the specimen grating was replicated onto the package surface at 85°C.

The moiré system was tuned at the grating replication temperature and the null field patterns were taken as shown in Fig. 8(a). The package was cooled to 25°C and the resulting thermal deformations were measured. The fringe patterns are shown in Fig. 8(b), which represent in-plane displacement maps, induced by  $\Delta T$  of -60°C.

The package was then subjected to 85°C/85%RH until the saturation state was achieved. The package was installed in the real-time moiré system at 85°C and the deformations caused by hygroscopic swelling at the saturation state were measured. The resulting fringe patterns are shown in Fig. 9(a). No reference specimen was used for this experiment since it was not practically possible to have two identical package specimens. Instead, the specimen grating was replicated from a special grating mold fabricated on an ultra-low expansion (ULE) glass. The ULE grating mold has a virtually zero  $CTE$ . This negligible  $CTE$  allowed the ULE grating to be used as a reference to set a null field at any temperature after moisture absorption [10][11].

The measurements were carried on while desorption process continued. Representative fringe patterns of the package at time interval of 8 hours are shown in Fig. 9(b). A significant contraction of the package is evident; the number of fringes in the package decreased significantly after 8 hours of desorption.

The fringe patterns at the zero hour (Fig. 9a) represent the hygroscopic mismatch deformation at the virtual saturation point. It is important to remember that the measurement was made at the grating replication temperature (85°C), and thus the fringe patterns shown in Fig. 9 represent deformations induced only by hygroscopic swelling and do not contain any thermally induced deformations.

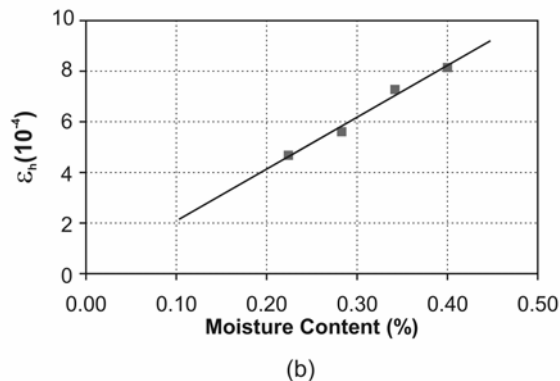
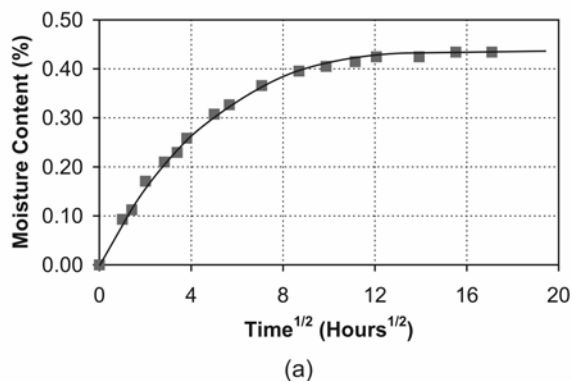


Fig. 10. (a) Sorption curve and (b) free hygroscopic strain vs. moisture content (%) of the mold compound of the package.

The displacement fields shown in Figs. 8 and 9 represent the total deformation of the package, which include the free thermal (Fig. 8) and the free hygroscopic (Fig. 9) part of the deformation and the stress-induced part of the deformation. Mathematically, the total strain of the package is

$$\text{For thermal strain: } \epsilon_{\alpha}^T = \epsilon_{\alpha}^f + \epsilon_{\alpha}^{\sigma} = \alpha \Delta T + \epsilon_{\alpha}^{\sigma} \quad (6)$$

$$\text{For hygroscopic strain: } \epsilon_{\beta}^T = \epsilon_{\beta}^f + \epsilon_{\beta}^{\sigma} = \beta C + \epsilon_{\beta}^{\sigma}$$

where  $\epsilon^T$  is the total strain,  $\epsilon^f$  is the free expansion/contraction part of strain,  $\epsilon^{\sigma}$  is the stress-induced part of the strain; the subscript of  $\alpha$  and  $\beta$  denotes the cases of thermal deformation and hygroscopic deformation, respectively.

The values of  $\alpha$  and  $\beta$  of the mold compound were not known. They were determined from the regions sufficiently far away from the chip (regions marked by dashed boxes in Fig. 7), where the deformations represent only  $\epsilon^f$  of the mold compound. The value of  $\alpha$  was determined from the fringe patterns in Fig. 8b and it was 14.4 (ppm/°C). The value of  $\beta$  was determined using the same procedure used for the mold compounds. Fringe patterns at various desorption times were analyzed, and the swelling in these regions was plotted versus moisture content. The sorption curve is shown in Fig. 10(a) and the result of swelling versus moisture content is shown in Fig. 10(b). The maximum moisture content and the  $CHS$  value were determined as  $C = 0.43\%$  and  $\beta = 0.21$  ( $\% \epsilon_h / \% C$ ), respectively. The  $CHS$  value was approximately

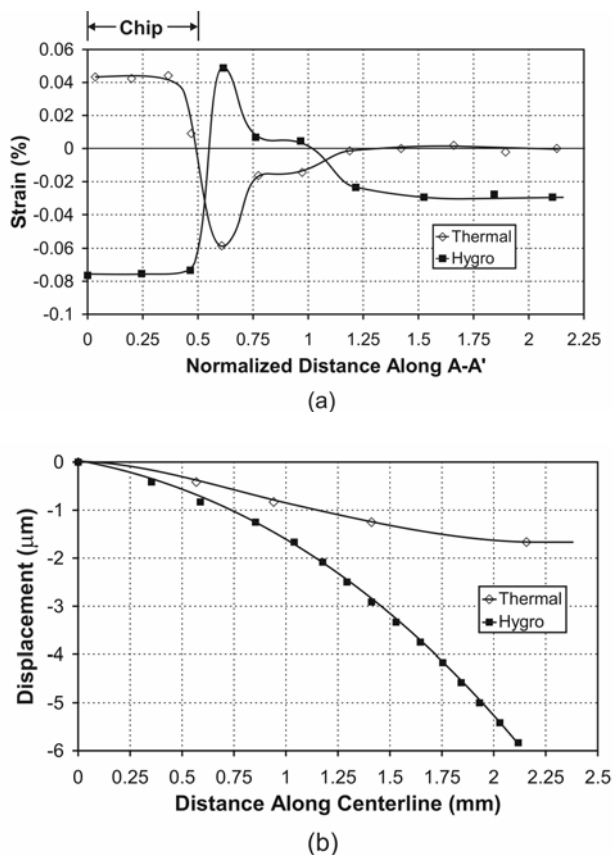


Fig. 11. (a) Stress-induced strains and (b) bending displacements along the chip/mold compound interface.

the same as the average value of the five mold compounds. The moisture content was similar to that of the two mold compounds with the higher moisture content.

The total  $x$  direction strains along a line just above the top of the chip were obtained directly from the  $U$  field fringe patterns. The corresponding stress-induced strains were then calculated using Eq. 6, with  $\Delta T = 60^\circ\text{C}$ , and  $C = 0.43\%$ . The results along the dashed line (AA' shown in Fig. 7) are plotted in Fig. 11a, where the  $x$ -axis represents a distance from the center of the package, normalized by the width of the chip. Along the chip/mold compound interface ( $x < 0.5$ ),  $\varepsilon_\alpha^\sigma$  is tensile while  $\varepsilon_\beta^\sigma$  compressive. The magnitude of the stress-induced strain caused by  $CHS$  mismatch,  $\varepsilon_\beta^\sigma$ , is nearly twice as large as that produced by the  $CTE$  mismatch,  $\varepsilon_\alpha^\sigma$ , with  $\Delta T$  of  $60^\circ\text{C}$ . The strains change abruptly around the edge of the chip. These were caused by the material discontinuity. The signs of the strains were reversed but their magnitudes reduced to a uniform value at about half the chip width from the edge of the chip.

Another interesting phenomenon was observed in the  $V$  displacement fields. The bending displacements along the line were determined from the  $V$  field fringe patterns, and they are plotted in Fig. 11b. Unlike the strains, the bending displacements have the same sign. The total bending displacement induced by swelling is nearly three times as

large as that by thermal deformation. The bending was caused by the fact that the lead-frame was not placed in the middle of the package. The  $CTE$  of copper lead frame ( $17 \text{ ppm}/^\circ\text{C}$ ) is reasonably close to that of the molding compound ( $14.4 \text{ ppm}/^\circ\text{C}$ ) and the  $CTE$  mismatch was not significant. However, the swelling coefficient of the leadframe is zero and the swelling mismatch caused a larger bending. The chip also contributed to the bending displacement but its effect was not significant because of its small relative volume.

## V. DISCUSSIONS

The above results show that hygroscopic swelling effects can have a significant impact on PEM reliability. The hygroscopic strains must be considered for reliability assessment in environments, such as in automotive applications, where packages are subjected to both temperature excursions and relative humidity changes. A SAE document [16] shows that electronic equipment is commonly subjected to a  $38^\circ\text{C}/95\%RH$  environment throughout the automobile, and environments of  $66^\circ\text{C}/80\%RH$  in multiple locations in the automobile.

Accelerated life testing conditions such as a HAST (Highly Accelerated Stress Test) chamber, where temperature, humidity, and pressure are used, may also witness complications due to hygroscopic swelling issues. The temperature conditions in a HAST chamber are typically from  $100^\circ\text{C}$  to  $150^\circ\text{C}$ , the relative humidity is typically over 70%, and the pressure can be up to 50 psi. These conditions will drastically increase the amount of moisture absorbed by the polymeric materials in a package, and therefore greatly increase the hygroscopic swelling.

It is well known that temperature changes and thermal expansion mismatches can cause stresses and deformations that can lead to reliability problems in PEMs. The experimental evidence here indicates that hygroscopic stresses can also have a significant impact on PEM reliability. In fact, this study shows that the hygroscopic swelling induced deformations can be larger than thermally induced deformations in some packages. Numerical analysis such as finite element analysis has been used extensively to assess reliability of microelectronics devices. The analysis must include predictive capabilities of hygroscopic swelling if relative humidity is present in the field condition.

## VI. CONCLUSION

A novel experimental procedure utilizing a whole-field displacement measurement technique was implemented to determine the coefficient of hygroscopic swelling of five commercially available mold compounds. The results showed significant variation (more than 100%) in the moisture content at the virtual equilibrium state but relatively small variation (less than 20%) in the coefficient of hygroscopic swelling.

The technique was also used to investigate an actual plastic package with a copper leadframe to evaluate the  $CHS$  mismatch strains. The results were compared with the  $CTE$  mismatch strains. The magnitude of the stress-induced strain

caused by *CHS* mismatch was nearly twice as large as that produced by *CTE* mismatch with  $T$  of  $60^{\circ}\text{C}$ . Although the magnitude of the *CHS* mismatch strain is not large, a significant strain gradient and thus a large stress gradient at the interface is expected since the strain of the chip is virtually zero. Hygroscopic strains must be considered for accurate reliability assessment when plastic packages are subjected to environments where the relative humidity fluctuates.

#### ACKNOWLEDGMENT

This work was supported by the CALCE Electronic Product and Systems Center of the University of Maryland. Their support is gratefully acknowledged. The authors also wish to thank Mr. Toru Kamei of Sumitomo Bakelite Co., Ltd. for providing the mold compounds used in this study.

#### REFERENCES

- [1] Pecht, M.G., Nguyen, L.T. and Hakim, E.B., *Plastic Encapsulated Microelectronics*, John Wiley & Sons, New York, 1995.
- [2] Ardebili, H., Wong, E.H. and Pecht, M., "Hygroscopic Swelling and Sorption Characteristics of Epoxy Molding Compounds Used in Electronic Packaging," *IEEE Transactions on Components and Packaging Technology*, Vol. 26, No. 1, pp. 206-214, 2003.
- [3] Toprak, C., Agar, J.N., and Falk, M., "State of Water in Cellulose Acetate Membranes," *Journal of Chemical Society, Faraday Trans I*, Vol. 75, pp. 803-815, 1979.
- [4] Chang, Y.J., Chen, C.T., and Tobolsky, A.V., "Correlations Between Types of Absorbed Water Molecules and Water Permeability in Swollen Polymer Members," *Journal of Polymer Science - Polymer Physics*, Vol. 12, pp. 1-6, 1974.
- [5] Ushitsky and M., Suhir, E., "Moisture Diffusion in Epoxy Molding Compounds Filled With Particles," *Journal of Electronic Packaging, Transaction of the ASME*, Vol. 123, pp. 47-51, 2001.
- [6] Adamson, M.J., "Thermal Expansion and Swelling of Cured Epoxy Resin Used in Graphite/Epoxy Composite Materials," *Journal of Materials Science*, Vol. 15, No. 7, pp. 1736-1745, 1980.
- [7] El'saad, L. Darby, M.I., and Yates, B., "Moisture Absorption by Epoxy Resins: The Reverse Thermal Effect," *Journal of Materials Science*, Vol. 25, No. 8, pp. 3577-3582, 1990.
- [8] Wong, E.H., Chan, K.C., Rajoo and R., Lim, T.B., "The Mechanics and Impact of Hygroscopic Swelling of Polymeric Materials in Electronic Packaging," Proceedings of the 50th Electronic Components and Technology Conference, Las Vegas, NV, pp. 576-580, 2000.
- [9] Stellrecht, E., Han, B. and Pecht, M., "Measurement of the Hygroscopic Swelling Coefficient in Mold Compounds Using Moiré Interferometry," *Experimental Techniques*, Vol. 27, No. 4, pp. 40-44, 2003.
- [10] Post, D., Han, B. and Ifju, P., *High Sensitivity Moiré: Experimental Analysis for Mechanics and Materials*, Mechanical Engineering Series, Springer-Verlag, NY, 1994. Also Post D., Han, B. and Ifju P., Chap. 7, "Moiré Methods for Engineering and Science – Moiré Interferometry and Shadow Moiré," *Photomechanics for Engineers*, Pramod Rastogi, ed., Springer-Verlag, 2000.
- [11] Han, B., "Recent Advancement of Moiré and Microscopic Moiré Interferometry for Thermal Deformation Analyses of Microelectronics Devices," *Experimental Mechanics*, Vol. 38, No. 4, pp. 278-288, 1998.
- [12] Han, B., Post, D. and Ifju, P., "Moiré Interferometry for Engineering Mechanics: Current Practice and Future Development," *Journal of Strain Analysis*, Vol. 36, No. 1, pp. 101-117, 2001.
- [13] Han, B., "Thermal Stresses in Microelectronics Subassemblies: Quantitative Characterization using Photomechanics Methods," *Journal of Thermal Stresses*, Vol. 26, pp. 583-613, 2003.
- [14] Cho, S.M., Cho, S.Y. and Han, B., "Observing Real-Time Thermal Deformations in Electronic Packaging," *Experimental Techniques*, Vol. 26, No. 3, pp. 25-29, 2002.
- [15] Stellrecht, E., "The Measurement of hygroscopic swelling In Plastic Encapsulated Microelectronics using Moiré Interferometry," *MS Thesis*, University of Maryland, 2003.
- [16] SAE, Recommended Environmental Practices for Electronics Equipment Design, Document #: J1211, Revised: November 1978.



**Eric Stellrecht** received his BS degree in Mechanical Engineering from Binghamton University in 2001 and his MS degree in Mechanical Engineering from the University of Maryland - College Park in 2003. He is now a member of the Mechanical Engineering staff at DRS – Electronic Warfare and Network Systems in Buffalo, NY. He has authored and co-authored several papers relating to hygroscopic swelling in the microelectronics industry.



**Bongtae Han** received his BS and MS degrees from Seoul National University and his Ph.D. degree in Engineering Mechanics from Virginia Polytechnic Institute & State University in 1991. He is currently an Associate Professor of the Mechanical Engineering Department of the University of Maryland at College Park and one of Research Directors at CALCE Electronic Products and Systems Center, directing the Laboratory for Opto-Mechanics and Multi-layer

Systems. His research interest is centered on design/process optimization of microelectronics devices for optimum mechanical reliability. His previous professional industrial career includes Advisory Engineer at IBM Microelectronics (1992-1996).

Dr. Han is responsible for development of Portable Engineering Moiré Interferometer, and holds a related patent. He has co-authored a text book entitled "High Sensitivity Moiré: Experimental Analysis for Mechanics and Materials", Springer-Verlag, 1994. He edited two books and has published over 90 journal and conference papers in the field of microelectronics and experimental mechanics. He served as an Executive Board Member and the Chairman of the Electronic Packaging Division of the Society for Experimental Mechanics (SEM). He served as an Associate Technical Editor for the international journal, *Experimental Mechanics*, from 1999 to 2001 and is currently serving as an Associate Technical Editor of *Journal of Electronic Packaging*, Transaction of the ASME. He holds a membership in ASME, IEEE, IMAPS and SPIE.

He received the *IBM Excellence Award for Outstanding Technical Achievements* in 1994. He was a recipient of the *2001 Brewer Award* at the Annual Conference of the SEM in Emerging Technologies for his contributions to experimental characterization of microelectronics devices.



**Michael Pecht** has a BS in Acoustics, an MS in Electrical Engineering and an MS and PhD in Engineering Mechanics from the University of Wisconsin at Madison. He is a Professional Engineer and an IEEE Fellow. He has received the 3M Research Award, the IEEE Undergraduate Teaching Award, and the IMAPS William D. Ashman Memorial Achievement Award for his contributions. He has written eighteen books on electronic products

development, use and supply chain management. He has also edited a series of books on the Asian electronics industry including a recent book titled "The Chinese Electronics Industry – 2004 edition." He served as chief editor of the IEEE Transactions on Reliability for eight years and on the advisory board of IEEE Spectrum. He is the founder and the Director of the CALCE Electronic Products and Systems Center at the University of Maryland and a Chair Professor. He is chief editor for Microelectronics Reliability and an associate editor for the IEEE Transactions on Components and Packaging Technology. He has consulted for over 50 major international electronics companies, providing expertise in strategic planning, design, test, IP and risk assessment of electronic products and systems.